PHYSICAL REVIEW B VOLUME 11, NUMBER 4 15 FEBRUARY 1975

# Density-functional theory of chemisorption on metal surfaces

S. C. Ying*
*Department of Physics, Brown University, Providence, Rhode Island 02912*

J. R. Smith
*Research Laboratories, General Motors Corporation, Warren, Michigan 48090*

W. Kohn†
*Department of Physics, University of California, San Diego, La Jolla, California 92037*
(Received 15 July 1974)

The density-functional theory of chemisorption is developed by means of a self-consistent linear-response formalism. Any chemisorbed species which can be represented as an external charge distribution perturbing the metallic surface can be studied with this approach. The formalism is applied to hydrogen chemisorbed on a tungsten surface. Theoretical results for the ionic desorption energy, adatom vibrational frequency, relative size of the dipole moment, resonance levels associated with the adsorbate, and the question of dissociation agree well with experimental measurements. The calculated level width is too large. Differential scattering cross sections for chemisorbed hydrogen are compared with those of the isolated atom. The rather satisfactory over-all agreement of our theory with experimental results suggests that the linear response formalism may have a wider usefulness.

## I. INTRODUCTION

Chemisorption on metals has lately been receiving increasing attention both by experimentalists and theorists. The reasons are the growing importance of such technological applications as catalysis, corrosion, and adhesion; the rapid development of new and improved methods for the experimental study of surfaces; and helpful developments in related areas of solid state theory.

Earlier theoretical work, following several different approaches, has been reviewed in a number of recent articles,[1] so that we shall be very brief here. The molecular-orbital approach using the Anderson (or sometimes Hubbard) Hamiltonian has been developed by Newns,[2] Grimley,[3] Bennett and Falicov,[4] Einstein and Schrieffer,[5] and others. These model theories, containing a small number of adjustable parameters, such as transfer-matrix elements and effective intra-atomic Coulomb repulsion, have been useful in giving qualitative and sometimes semiquantitative insights into the phenomenon of chemisorption. Cyrot-Lackmann[6] and collaborators have used a moment method for evaluating single-particle densities of states in the tight-binding version of the molecular-orbital model. Another approach has been explored by Schrieffer and Gomer,[7] who start from a picture analogous to the Heitler-London theory of covalent molecular binding. Subsequent developments along this line have not yet appeared in the literature. Extended Hückel theory, a semiempirical molecular-orbital technique, has been applied (see, e.g., Anders[8] *et al.*) to investigate structural effects. In all these theories, electrostatic self-consistency has generally been disregarded; occasional efforts at ensuring charge neutrality have been made.

We present here a method which allows full electrostatic self-consistency. This has been found to be very important for both clean metal surfaces and in the screening of charges in the surface region. Although a number of simplifying assumptions are made, no adjustable parameters are introduced. The assumptions are the following: (i) The substrate (e.g., W) is represented by a jellium model with appropriate positive-charge density. (ii) The density functional $G[n]$, appearing in the expression for the electronic energy, is represented by the first two terms of the gradient expansion, valid for slow variation of the density $n$. (iii) The perturbation due to the chemisorbed entity is treated in linear approximation. These assumptions are discussed in the remaining sections and appendices of this paper.

In Sec. II, the general linear screening formalism in the density-functional formalism, which has been presented in an earlier publication,[9] is reviewed. In Sec. III, the explicit form of the response function is obtained in the gradient-expansion approximation of the energy functional. The asymptotic behavior of the induced potential and the derivation of the image potential and image plane are presented in Sec. IV. In Sec. V the formalism is applied to hydrogen chemisorption.[10] Various observable quantities such as the ionic desorption energy, induced dipole moment, adatom vibrational frequency, resonance level and width, and differential electron scattering cross sections are calculated. It will be shown that the theoretical values on the whole compare favorably with available ex-

perimental data. In addition, the calculated charge densities and potentials allow visualization of the chemisorption process.

## II. REVIEW OF GENERAL LINEAR-RESPONSE FORMALISM

In this section we review the formalism of the dielectric response in the density-functional approach.[9] Consider first an unperturbed inhomogeneous electron gas at $T=0^\circ$, in an external potential $V_0^{ex}(\vec{r})$ and with electron number density $n_0(\vec{r})$. Now introduce an additional small charge density $\rho_1^{ex}(\vec{r})$ giving rise to a perturbing potential

$$V_1^{ex}(\vec{r}) = \int \frac{\rho_1^{ex}(\vec{r}\,')}{|\vec{r}-\vec{r}\,'|}\, d\vec{r}\,' \tag{2.1}$$

(we use atomic units unless stated otherwise). What is the resulting change $n_1(\vec{r})$ of the electronic density?

According to Hohenberg and Kohn[11] there exists a universal functional of the density $G[n(\vec{r})]$ such that the density $n(\vec{r})$ corresponding to any given $V^{ex}(\vec{r})$ is determined by the requirement that it minimizes the energy functional

$$E[n] = -\int V^{ex}(\vec{r})n(\vec{r})\, d\vec{r} + \frac{1}{2}\int \frac{n(\vec{r})n(\vec{r}\,')}{|\vec{r}-\vec{r}\,'|} d\vec{r}\, d\vec{r}\,' + G[n], \tag{2.2}$$

subject to the condition that the total number of electrons remains constant. Introducing the latter condition through a Lagrange multiplier $\mu$ gives

$$-V(\vec{r}) + \frac{\delta G[n]}{\delta n(\vec{r})} = \mu, \tag{2.3}$$

where $V(\vec{r})$ is the total electrostatic potential

$$V(\vec{r}) = V^{ex}(\vec{r}) - \int \frac{n(\vec{r}\,')}{|\vec{r}-\vec{r}\,'|}\, d\vec{r}\,' \tag{2.4}$$

and $\mu$ is the chemical potential. Equations (2.3) and (2.4) determine $n$ and $V$. Now linearizing (2.3) and (2.4), i.e., writing $V^{ex} = V_0^{ex} + V_1^{ex}$, $n = n_0 + n_1$, etc., gives the following results. The zeroth-order density is determined by the equations

$$-V_0(\vec{r}) + \frac{\delta G[n]}{\delta n(\vec{r})}\bigg|_{n(\vec{r})=n_0(\vec{r})} = \mu_0, \tag{2.5}$$

$$V_0(\vec{r}) = V_0^{ex}(\vec{r}) - \int \frac{n_0(\vec{r}\,')}{|\vec{r}-\vec{r}\,'|} d\vec{r}\,'; \tag{2.6}$$

and the first-order screening density is given by

$$-V_1(\vec{r}) + \int n_1(\vec{r}\,') \frac{\delta^2 G[n]}{\delta n(\vec{r})\delta n(\vec{r}\,')}\bigg|_{n=n_0} d\vec{r}\,' = \mu_1, \tag{2.7}$$

$$V_1(\vec{r}) = V_1^{ex}(\vec{r}) - \int \frac{n_1(\vec{r}\,')}{|\vec{r}-\vec{r}\,'|} d\vec{r}\,'. \tag{2.8}$$

A calculation of $n_1(\vec{r})$ then proceeds as follows: The solution of (2.5) and (2.6) gives $n_0$ and $V_0$; these quantities are then used in (2.7) and (2.8) to determine $n_1$ and $V_1$. We define the density-potential response function $L(\vec{r}, \vec{r}\,')$ by the equation

$$V_1(\vec{r}) = \int L(\vec{r}, \vec{r}\,')\rho_1^{ex}(\vec{r}\,')\, d\vec{r}\,' \tag{2.9}$$

and the density-density response function $R(\vec{r}, \vec{r}\,')$ by the equation

$$n_1(\vec{r}) = \int R(\vec{r}, \vec{r}\,')\rho_1^{ex}(\vec{r}\,')\, d\vec{r}\,'. \tag{2.10}$$

$L(\vec{r}, \vec{r}\,')$ and $R(\vec{r}, \vec{r}\,')$ can be determined by finding the induced potential $V_1(\vec{r})$ and electronic density $n_1(\vec{r})$ due to an external perturbing charge of the form $\rho_1^{ex}(\vec{r}) = \delta(\vec{r}-\vec{r}\,')$. This is described in Sec. III. Once these response functions are determined they can be used in Eqs. (2.9) and (2.10) to study the response to a general external charge distribution corresponding to chemisorbed species.

Note that it follows immediately from the Hellmann-Feynman theorem and linearity that

$$L(\vec{r}, \vec{r}\,') = L(\vec{r}\,', \vec{r}); \tag{2.11}$$

that is, the density-potential response function obeys *reciprocity*.

## III. SCREENING IN A METALLIC SURFACE

The general formalism for dielectric screening in an inhomogeneous gas is now applied to a metallic surface. The unperturbed metal is described by the jellium model:

$$\rho_0^{ex}(\vec{r}) = \rho_+\theta_-(x), \tag{3.1}$$

where

$$\theta_-(x) = \begin{cases} 1, & x \le 0 \\ 0, & x > 0. \end{cases} \tag{3.2}$$

In Ref. 9 the response functions were derived in the simplest possible approximation for the functional $G[n]$, the Thomas-Fermi expression

$$G[n] = \tfrac{3}{10}(3\pi^2)^{2/3}\int n^{5/3}(\vec{r})\, d\vec{r}. \tag{3.3}$$

This is the crudest form of a more general gradient expansion,[11]

$$G[n] = \int g_0(\vec{r})\, d\vec{r} + \int g_2(\vec{r})\,|\vec{\nabla} n(\vec{r})|^2 d\vec{r} + \cdots \tag{3.4}$$

which incorporates approximately many-body and inhomogeneity effects.

The simple, analytic Thomas-Fermi response function is particularly useful in the high-density limit. However, it does have the unsatisfactory feature that the dipole moment is always zero:

$$\int n_1(\vec{r})(x-x')\, d\vec{r} = 0. \tag{3.5}$$

To attain a better description for the screening of external charges at metallic densities, we use the more accurate energy functional:

$$G[n]=\tfrac{3}{10}(3\pi^2)^{2/3}\int n^{5/3}d\vec{r}-\tfrac{3}{4}(3/\pi)^{1/3}\times\int n^{4/3}d\vec{r}+\frac{1}{72}\int\frac{(\vec{\nabla}n)^2}{n}\,d\vec{r}\,. \tag{3.6}$$

This choice of $G[n]$ is known to work very well for bare-surface properties, such as work-function and density contours.[12] This form omits the correlation contribution to $g_0(\vec{r})$ and the exchange and correlation contributions to $g_2(\vec{r})$. For densities occurring in the present application the omitted terms are believed to be small (see Ref. 13 and Appendix B). The last term in Eq. (3.6) describes the inhomogeneity correction of the kinetic energy for sufficiently slowly varying density. It is shown in Appendix A that this condition is probably adequately satisfied. This is the second approximation listed in Sec. I.

The third approximation is that of linear response. The applicability of linear-response theory to the screening of a finite point charge in a metal surface has been investigated by Appelbaum and Hamann[14] via a variational calculation. They found excellent scaling as $z^2$ for the interaction energy between the charge $z$ and a (jellium) metal surface. $z$ values up to 2 and metal point-charge separations as small as 1 a.u. were considered. This supports the use of the linear approximation in chemisorption. For further discussion see Appendix A.

With the $G[n]$ of Eq. (3.6), we have

$$\frac{\delta G[n]}{\delta n(\vec{r})}=\tfrac{1}{2}(3\pi^2)^{2/3}n^{2/3}(\vec{r})-(3/\pi)^{1/3}n^{1/3}(\vec{r})+\tfrac{1}{72}[\nabla n(\vec{r})]^2-\frac{1}{36n(\vec{r})}\nabla^2 n(\vec{r}) \tag{3.7}$$

and

$$\frac{\delta^2 G}{\delta n(\vec{r})\delta n(\vec{r}')}=\tfrac{1}{3}\delta(\vec{r}-\vec{r}')\Big[(3\pi^2)^{2/3}n^{-1/3}(\vec{r})-(3/\pi)^{1/3}n^{-2/3}(\vec{r})-\frac{|\nabla' n(\vec{r}')|^2}{12n^3(\vec{r})}+\frac{\nabla'^2 n(\vec{r}')}{12n^2(\vec{r})}\Big]+[\vec{\nabla}'\delta(\vec{r}'-\vec{r})]\frac{1}{36n^2}\nabla' n(\vec{r}')-[\nabla'^2\delta(\vec{r}'-\vec{r})]\frac{1}{36n(\vec{r})}\,. \tag{3.8}$$

As the unperturbed system is one dimensional, it is convenient to introduce the two-dimensional Fourier transform of various quantities parallel to the surface in the form

$$L(Q,\,x;\,x')=\int d\vec{u}\,e^{-i\vec{Q}\cdot\vec{u}}L(u,\,x;\,x') \tag{3.9}$$

and

$$n_1(Q,\,x;\,x')=\int d\vec{u}\,e^{-i\vec{Q}\cdot\vec{u}}n_1(u,\,x;\,x'),$$

etc., where

$$\vec{Q}\equiv(0,\,Q_y,\,Q_z),\quad \vec{u}\equiv(0,\,y-y',\,z-z'),$$
$$u\equiv|\vec{u}|,\quad Q\equiv|\vec{Q}|\,.$$

Substituting (3.7) and (3.8) into (2.5) and (2.7) and Fourier transforming all quantities as indicated by (3.9) we arrive at the equations

$$\frac{d^2}{dx^2}V_1(Q,\,x)-Q^2V_1(Q,\,x)=4\pi[n_1(Q,\,x)-\delta(x-x')] \tag{3.10}$$

and

$$-\frac{1}{36n_0(x)}\frac{d^2n_1(Q,\,x)}{dx^2}+\left(\frac{dn_0(x)}{dx}\Big/36n_0^2(x)\right)\frac{dn_1(Q,\,x)}{dx}+\left(X+\frac{Q^2}{36n_0(x)}\right)n_1(Q,\,x)-V_1(Q,\,x)=\mu_1\delta(Q)\,, \tag{3.11}$$

where

$$X=\tfrac{1}{3}(3\pi^2)^{2/3}n_0^{-1/3}(x)-\tfrac{1}{3}(3/\pi)^{1/3}n_0^{-2/3}(x)-\frac{[\nabla n_0(x)]^2}{36n_0^3(x)}+\frac{\nabla^2 n_0(x)}{36n_0^2(x)}\,. \tag{3.12}$$

It is convenient at this point to scale the charge density in units of $(e/a_0^3)(\frac{4}{3}\pi r_s^3)^{-1}$ and distance in units of $a_0(\frac{3}{128}\pi^2)^{1/6}r_s^{1/2}$. With this scaling, Poisson's equation becomes

$$V_1''(Q,\,x)-Q^2V_1(Q,\,x)=n_1(Q,\,x)-\delta(x-x')\,. \tag{3.13}$$

For $x\neq x'$, one can combine Eqs. (3.13) and (3.11) to yield

$$V_1''''(Q,\,x)-\frac{n_0'(x)}{n_0(x)}V_1'''(Q,\,x)+(Y-2Q^2)V_1''(Q,\,x)+\frac{n_0'(x)}{n_0(x)}Q^2V_1'(Q,\,x)+[k_h n_0(x)-Q^2Y+Q^4]V_1(Q,\,x)=k_h n_0(x)\mu_1\delta(\vec{Q})\,,$$

where

$$Y=\left(\frac{n_0'(x)}{n_0(x)}\right)^2-\frac{n_0''(x)}{n_0(x)}+\tfrac{9}{2}n_0^{1/3}(x)-\tfrac{2}{3}k_h n_0^{2/3}(x)\,,\qquad k_h=r_s^{-1}\pi^{4/3}3^{11/3}2^{-8/3}\,. \tag{3.14}$$

and primes denote differentiation with respect to $x$.

The solution to $V_1$ in the presence of the external perturbation is obtained by imposing on the solutions of (3.14) the following boundary conditions:

$$\begin{aligned}&V_1(Q,\,\pm\infty)=0\,,\\ &n_1(Q,\,x_+')=n_1(Q,\,x_-')\,,\\ &n_1'(Q,\,x_+')=n_1'(Q,\,x_-')\,,\\ &V_1(Q,\,x_+')=V_1(Q,\,x_-')\,,\\ &V_1'(Q,\,x_+')-V_1'(Q,\,x_-')=-1\,.\end{aligned} \tag{3.15}$$

To solve (3.14) we note some general conditions

that must be satisfied by $n_1$ and $V_1$: (a) Integration of Poisson's equations gives

$$V_1'(Q=0,\ \infty) - V_1'(Q=0,\ -\infty) = -1 + \int_{-\infty}^{\infty} n_1(Q=0,\ x)\,dx. \tag{3.16}$$

Since $V_1'(Q=0,\ \infty) = V_1'(Q=0,\ -\infty) = 0$,

$$\int_{-\infty}^{\infty} n_1(Q=0,\ x)\,dx = 1\,. \tag{3.17}$$

This is the charge-neutrality requirement. (b) Again, multiplying the Poisson's equation by $(x-x')$ and integrating by parts, we obtain

$$V_1(Q=0,\ -\infty) - V_1(Q=0,\ \infty) = \int_{-\infty}^{\infty} n_1(Q=0,\ x)(x-x')\,dx\,. \tag{3.18}$$

Because $n_1(Q,\ x)$ is a continuous function of $Q$, (3.18) can also be written

$$V_1(Q=0,\ -\infty) - V_1(Q=0,\ \infty) = \lim_{Q\to 0} \int_{-\infty}^{\infty} n_1(Q,\ x)(x-x')\,dx\,. \tag{3.19}$$

In contrast to the Thomas-Fermi approximation, the dipole moment given by (3.19) is in general nonvanishing. It is important to note that $V_1(Q=0,\ \infty)$ and $V_1(Q=0,\ -\infty)$ appearing in Eqs. (3.16), (3.17), (3.18), and (3.19) should be understood as $\lim_{x\to\pm\infty}\lim_{Q\to 0} V_1(Q,\ x)$. The order in which the limit is taken cannot be interchanged.

To obtain the response function, we shall first solve for the independent solutions of (3.14) in the absence of external perturbation by a procedure similar to that which was used to obtain the Thomas-Fermi solution.[9] The various coefficients in the differential equations are represented approximately by finite polynomials of a new variable $t$ which is defined as

$$\begin{aligned} t &= e^{-\beta_R x} \quad \text{for } x>0\,, \\ t &= e^{\beta_L x} \quad \text{for } x<0\,. \end{aligned} \tag{3.20}$$

The parameters $\beta_R$ and $\beta_L$ are chosen to yield a best fit. This is motivated by the fact that for $r_s \le 4$ the solution $n_0$ obtained by Lang and Kohn[13] is very close to the simple variational solution employed by Smith,[12]

$$n_0(x) = \tfrac{1}{2}\Theta(x)e^{-\beta x} + \tfrac{1}{2}\Theta(-x)(1-e^{\beta x})\,.$$

Thus, in this work the data of Lang and Kohn[13] are fitted to finite polynomials of the new variable $t$. It is found that, when $r_s = 1.5$, a two-term polynomial on each side of $x=0$ fits the function $n_0^{1/3}(x)$ to within 1% of $\rho+$ for all values of $x$. The coefficients of the differential equations can then be expressed in the form

$$V_1''''(Q,\ x) - B[V_1''(Q,\ x) - Q^2 V_1(Q,\ x)] + (C-2Q^2)V_1''(Q,\ x) + (k_h D - Q^2 C + Q^4)V_1(Q,\ x) = 0, \tag{3.21}$$

where

$$B = \sum_{n=0}^{N_0} B_n t^n, \quad C = \sum_{n=0}^{N_0} C_n t^n, \quad D = \sum_{n=0}^{N_0} D_n t^n\,.$$

With this change of variables from $x$ to $t$ the two points at $x = \pm\infty$ are now regular singular points of the differential equation (3.21), and a series solution of $V_1$ that converges for all values of $t$ between 0 and 1 can be written in the form

$$V_1(x) = t^s \sum_{n=0}^{\infty} a_n(s) t^n\,, \tag{3.22}$$

where the $a_n(s)$ satisfy a recurrence relation

$$a_n(s) = \frac{-\sum_{j=1}^{n}[-\beta^3(n-j+s)^3 B_j + C_j\beta^2(n-j+s)^2 + \beta Q^2(n-j+s)B_j]a_{n-j}}{\beta^4(s+n)^4 - B_0\beta^3(s+n)^3 + (C_0-2Q^2)\beta^2(s+n)^2 + B_0\beta Q^2(s+n) + Q^4 - Q^2C_0 + k_h D_0}\,. \tag{3.23}$$

The condition that $a_0 \neq 0$ determines $s$:

$$\beta^4 s^4 - B_0\beta^3 s^3 + (C_0 - 2Q^2)\beta^2 s^2 + B_0\beta Q^2 s + (Q^4 - Q^2 C_0 + k_h D_0) = 0\,. \tag{3.24}$$

For $x>0$, the four solutions are

$$\begin{aligned} s_1^+ &= \tfrac{3}{2}[1 + (1 + 4Q^2/9\beta_R^2)^{1/2}]\,, \\ s_2^+ &= Q/\beta_R\,, \\ s_3^+ &= \tfrac{3}{2}[1 - (1 + 4Q^2/9\beta_R^2)^{1/2}], \\ s_4^+ &= -Q/\beta_R\,, \end{aligned} \tag{3.25}$$

leading to four solutions for $V_1(x)$, $[u_1(x), \ldots, u_4(x)]$ and for $x<0$, (3.24) has the solutions

$$\begin{aligned} s_1^- &= (1/\beta_L)Q^2 + (\tfrac{1}{3}k_h - \tfrac{9}{4}) + (\tfrac{1}{3}k_h - \tfrac{9}{4})^2 - k_h\,, \\ s_2^- &= (1/\beta_L)Q^2 + (\tfrac{1}{3}k_h - \tfrac{9}{4}) - (\tfrac{1}{3}k_h - \tfrac{9}{4})^2 - k_h\,, \\ s_3^- &= -r_2\,, \\ s_4^- &= -r_1\,, \end{aligned} \tag{3.26}$$

leading to four solutions for $V_1(x)$, $[W_1(x), \ldots, W_4(x)]$.

The response of the system in the presence of the external perturbation now can be obtained by linear combination of these solutions to satisfy the boundary conditions. There are two different situations. For $x'>0$, i.e., external charge situated

outside the jellium surface, we have

$$L(Q,\ x,\ x') \equiv V_1(Q,\ x,\ x') = \begin{cases} \alpha_1 u_1 + \alpha_2 u_2, & x > x' \\ \beta_1 W_1 + \beta_2 W_2, & x < 0 \\ \gamma_1 u_1 + \gamma_2 u_2 + \gamma_3 u_3 + \gamma_4 u_4, & 0 < x < x' . \end{cases} \tag{3.27}$$

The coefficients $\alpha$, $\beta$, and $\gamma$ are obtained by solving the simultaneous equations

$$\begin{aligned}
&(\alpha_1-\gamma_1)u_1(Q,\ x') + (\alpha_2-\gamma_2)u_2(Q,\ x') - \gamma_3 u_3(Q,\ x') - \gamma_4 u_4(Q,\ x') = 0 , \\
&(\alpha_1-\gamma_1)u_1'(Q,\ x') + (\alpha_2-\gamma_2)u_2'(Q,\ x') - \gamma_3 u_3'(Q,\ x') - \gamma_4 u_4'(Q,\ x') = -1 , \\
&(\alpha_1-\gamma_1)u_1''(Q,\ x') + (\alpha_2-\gamma_2)u_2''(Q,\ x') - \gamma_3 u_3''(Q,\ x') - \gamma_4 u_4''(Q,\ x') = 0 , \\
&(\alpha_1-\gamma_1)u_1'''(Q,\ x') + (\alpha_2-\gamma_2)u_2'''(Q,\ x') - \gamma_3 u_3'''(Q,\ x') - \gamma_4 u_4'''(Q,\ x') = -Q^2 , \\
&\gamma_1 u_1(Q,\ 0) + \gamma_2 u_2(Q,\ 0) - \beta_1 W_1(Q,\ 0) - \beta_2 W_2(Q,\ 0) = -\gamma_3 u_3(Q,\ 0) - \gamma_4 u_4(Q,\ 0) , \\
&\gamma_1 u_1'(Q,\ 0) + \gamma_2 u_2'(Q,\ 0) - \beta_1 W_1'(Q,\ 0) - \beta_2 W_2'(Q,\ 0) = -\gamma_3 u_3'(Q,\ 0) - \gamma_4 u_4'(Q,\ 0) , \\
&\gamma_1 u_1''(Q,\ 0) + \gamma_2 u_2''(Q,\ 0) - \beta_1 W_1''(Q,\ 0) - \beta_2 W_2''(Q,\ 0) = -\gamma_3 u_3''(Q,\ 0) - \gamma_4 u_4''(Q,\ 0) , \\
&\gamma_1 u_1'''(Q,\ 0) + \gamma_2 u_2'''(Q,\ 0) - \beta_1 W_1'''(Q,\ 0) - \beta_2 W_2'''(Q,\ 0) = -\gamma_3 u_3'''(Q,\ 0) - \gamma_4 u_4'''(Q,\ 0) .
\end{aligned} \tag{3.28}$$

For $x' < 0$, we obtain instead

$$L(Q,\ x,\ x') = \begin{cases} \alpha_1 u_1 + \alpha_2 u_2 , & x > 0 \\ \beta_1 W_1 + \beta_2 W_2 , & x < x' \\ -\gamma_1 W_1 - \gamma_2 W_2 - \gamma_3 W_3 - \gamma_4 W_4 , & x' < x < 0 . \end{cases} \tag{3.29}$$

The $\alpha$, $\beta$, and $\gamma$ are now determined by the simultaneous equations

$$\begin{aligned}
&(\beta_1+\gamma_1)W_1(Q,\ x') + (\beta_2+\gamma_2)W_2(Q,\ x') + \gamma_3 W_3(Q,\ x') + \gamma_4 W_4(Q,\ x') = 0 , \\
&(\beta_1+\gamma_1)W_1'(Q,\ x') + (\beta_2+\gamma_2)W_2'(Q,\ x') + \gamma_3 W_3'(Q,\ x') + \gamma_4 W_4'(Q,\ x') = 1 , \\
&(\beta_1+\gamma_1)W_1''(Q,\ x') + (\beta_2+\gamma_2)W_2''(Q,\ x') + \gamma_3 W_3''(Q,\ x') + \gamma_4 W_4''(Q,\ x') = 0 , \\
&(\beta_1+\gamma_1)W_1'''(Q,\ x') + (\beta_2+\gamma_2)W_2'''(Q,\ x') + \gamma_3 W_3'''(Q,\ x') + \gamma_4 W_4'''(Q,\ x') = Q^2 , \\
&\alpha_1 u_1(Q,\ 0) + \alpha_2 u_2(Q,\ 0) + \gamma_1 W_1(Q,\ 0) + \gamma_2 W_2(Q,\ 0) = -\gamma_3 W_3(Q,\ 0) - \gamma_4 W_4(Q,\ 0) , \\
&\alpha_1 u_1'(Q,\ 0) + \alpha_2 u_2'(Q,\ 0) + \gamma_1 W_1'(Q,\ 0) + \gamma_2 W_2'(Q,\ 0) = -\gamma_3 W_3'(Q,\ 0) - \gamma_4 W_4'(Q,\ 0) , \\
&\alpha_1 u_1''(Q,\ 0) + \alpha_2 u_2''(Q,\ 0) + \gamma_1 W_1''(Q,\ 0) + \gamma_2 W_2''(Q,\ 0) = -\gamma_3 W_3''(Q,\ 0) - \gamma_4 W_4''(Q,\ 0) , \\
&\alpha_1 u_1'''(Q,\ 0) + \alpha_2 u_2'''(Q,\ 0) + \gamma_1 W_1'''(Q,0) + \gamma_2 W_2'''(Q,0) = -\gamma_3 W_3'''(Q,0) - \gamma_4 W_4'''(Q,0) .
\end{aligned} \tag{3.30}$$

## IV. ASYMPTOTIC SOLUTIONS: BULK SCREENING AND IMAGE POTENTIALS

From (3.23), (3.25), (3.27), and (3.28) it follows after some tedious algebraic manipulation that in the limit $x \gg 1$, $x' \gg 1$, $L(Q,\ x,\ x')$ takes the simple form

$$L(Q,\ x,\ x') = \frac{A(Q)}{2Q} e^{-Q(x+x')} + \frac{1}{2Q} e^{-Q|x-x'|} , \tag{4.1}$$

where

$$A(Q) = -\frac{\begin{vmatrix} W_1 & W_2 & u_2 & u_4 \\ W_1' & W_2' & u_2' & u_4' \\ W_1'' & W_2'' & u_2'' & u_4'' \\ W_1''' & W_2''' & u_2''' & u_4''' \end{vmatrix}}{\begin{vmatrix} W_1 & W_2 & u_1 & u_2 \\ W_1' & W_2' & u_1' & u_2' \\ W_1'' & W_2'' & u_1'' & u_2'' \\ W_1''' & W_2''' & u_1''' & u_2''' \end{vmatrix}} , \tag{4.2}$$

with all arguments of the functions evaluated at $x=0$. Inspection of Eq. (3.13) shows that Eq. (4.1) follows whenever $n_1(Q, x)\to 0$ faster in $x$ than does $V_1(Q, x)$.

The second term in (4.1) is just the contribution to $V_1$ due to the bare perturbing charge. The term proportional to $A(Q)$ corresponds to the induced potential. Closer examination of the recurrence relation (3.23) and the various indices for the series $u_1$–$u_4$ indicates that in the limit $Q\to 0$, $A(Q)$ has the following expansion in powers of $Q$:

$$A(Q)=-[1+Qd+O(Q^2)]. \tag{4.3}$$

This form also follows from charge neutrality [$\lim_{Q\to 0} L(Q, x; x')$ must be finite]. Thus at $x=x'$, the induced potential is given by

$$\bar{V}_1(Q, x=x')=-(1+Qd)e^{-2Qx'}/2Q . \tag{4.4}$$

The potential in real space is given by

$$\bar{V}_1(x=x', u)=\frac{1}{2\pi}\int_0^\infty \bar{V}_1(Q, x=x')J_0(Qu)Q\,dQ . \tag{4.5}$$

Thus the induced potential at the position of the point charge is given by

$$\bar{V}_1(x=x', u=0)=-\frac{1}{4\pi}\int_0^\infty dQ\,(1+Qd)e^{-2Qx'} =-\frac{1}{2\pi}\left[\frac{1}{4(x'-x_0)}+O\left(\frac{1}{x^3}\right)\right], \tag{4.6}$$

where $x_0=d/2$.

Asymptotically the induced potential indeed has the classical image-potential form; the plane $x=x_0$ acts as the effective position of the metallic surface. To investigate further the significance of $x_0$, we study again equation (4.1) in the limit $x\to\infty$, $Q\to 0$, and $Qx\to 0$. After a little algebra, one obtains

$$\lim_{x\to\infty}\lim_{Q\to 0} V_1(Q, x; x')=x'-x_0 . \tag{4.7}$$

It is also clear from the asymptotic properties of $W_1(x)$ and $W_2(x)$ that

$$V_1(Q=0, x\to-\infty, x')=0 . \tag{4.8}$$

Combining (4.7), (4.8), and (3.19) we arrive at the important result

$$x_0=\int_{-\infty}^{\infty} n_1(Q=0, x, x'=\infty)x\,dx . \tag{4.9}$$

Thus $x_0$ is exactly the center of mass of the induced charge. This result has been obtained by Lang and Kohn[15] on a more general basis. Our result (4.6) and (4.9) is an explicit verification of this fact within the present model of $G[n]$.

Next we investigate another asymptotic region, that corresponding to $x'\ll 0$. After some tedious algebra, one obtains from (3.29) and (3.30) the following result:

$$V_1=\frac{1}{2\beta_L r_1}a(r_s)e^{-r_1\beta_L(x-x')}+\frac{1}{2\beta_L r_2}[1-a(r_s)] \times e^{-r_2\beta_L|x-x'|} , \tag{4.10}$$

where $r_1$, and $r_2$ are given by (3.26) and

$$a(r_s)=\frac{[(k_h-\frac{27}{4})^2-9k_h]^{1/2}-(k_h-\frac{27}{4})}{2[(k_h-\frac{27}{4})^2-9k_h]^{1/2}} . \tag{4.11}$$

The three-dimensional potential is given by the formula

$$V_1(x, x', u)=\frac{1}{2\pi}\int_0^\infty V_1(Q, x, x')J_0(Qu)Q\,dQ . \tag{4.12}$$

Substitution of (4.10) into (4.12) yields the result

$$V_1(r)=\frac{1}{4\pi r}\{a(r_s)e^{-\lambda_1 r}+[1-a(r_s)]e^{-\lambda_2 r}\} . \tag{4.13}$$

As expected, the screening in this situation is spherically symmetric, corresponding to bulk behavior, and depends only on the variable

$$r=[(x-x')^2+u^2]^{1/2} .$$

Here

$$\lambda_1^2=\tfrac{1}{3}k_h-\tfrac{9}{4}+[(\tfrac{1}{3}k_h-\tfrac{9}{4})^2-k_h]^{1/2} \tag{4.14}$$

and

$$\lambda_2^2=\tfrac{1}{3}k_h-\tfrac{9}{4}-[(\tfrac{1}{3}k_h-\tfrac{9}{4})^2-k_h]^{1/2} .$$

In the limit $r_s\to 0$; $\lambda_1\to\infty$ and $\lambda_2^2\to\frac{3}{2}$, and we recover the Thomas-Fermi solution as expected. The induced density in $n_1(\vec{r})=\nabla^2 v_1(\vec{r})+\delta(\vec{r})$ at $r=0$ is given by

$$n_1(r=0)=\{-\lambda_1^3 a(r_s)-\lambda_2^3[1-a(r_s)]\}/4\pi . \tag{4.15}$$

We note that $n_1(r=0)$ is finite for finite $r_s$ but diverges as $r_s\to 0$, which corresponds to the well-known result that in the Thomas-Fermi approximation, the screening charge density at the position of the perturbing charge is infinite. Our solution at finite $r_s$ does not suffer from this defect.

## V. APPLICATION TO HYDROGEN CHEMISORPTION

Hydrogen chemisorption on metal surfaces is well studied experimentally (see, e.g., Refs. 16–19). Any theoretical description must be in accord with experimental heats of adsorption, changes in work function, adsorbate structure, desorption kinetics, photoemission energy distributions, and vibrational states of the adatom.

An important feature of our method is the requirement that Poisson's equation be satisfied point by point. That is, there is complete self-consistency between the electrostatic potential used and the charge density obtained. Such self-consistency is now established as essential in metal-surface calculations. In this section we regard a chemisorbed hydrogen atom as a proton dissolved in the inhomo-

TABLE I. Hydrogen chemisorbed on tungsten.

| | Theory | Expt. |
|---|---|---|
| Ion desorption energy (eV) | 9 | 11.3[a] |
| Dipole moment | small | small[b] |
| Resonance level (eV) | 5.6 | 5.7[c] |
| | | 6.3[c] |
| Vibrational energy (meV) | 200 | 140[d] |
| Adsorbed species | dissociated | dissociated[e] |

[a]References 21 and 22.
[b]Reference 17.
[c]Experimental values for the peak location below the Fermi level are taken from Ref. 10 (see also Ref. 11). The 5.7-eV value is for W(100), while the 6.3-eV result pertains to W(110).
[d]References 17 and 23.
[e]Reference 16.

geneous electron gas in the metallic-surface region and apply the screening formalism developed in the previous sections to study a considerable number of observed quantities.

The choice of the jellium model ($r_s = 1.5$) for the substrate is at once a strength and an apparent weakness of the calculation. Its strength is that it allows computation of all hydrogen chemisorption characteristics of interest from first principles with no adjustable parameters. It has an apparent weakness when applied to a transition metal like tungsten. However, over the last few years it has been found that those surface properties which depend primarily on the "tail" of the electron number density distribution appear not to be extremely sensitive to the details of the substrate model.[20] By the tail we mean that portion of $n(\vec{r})$ representing electrons which have tunneled part way into the vacuum region. Thus we conclude that we have a good zeroth-order model for chemisorption for the low-index planes of a refractory transition metal.

In the remainder of this section, results are given for a number of observables. A partial summary is contained in Table I.

### A. Ion-metal interaction energy

The interaction energy between the hydrogen ion and the metal substrate is to be determined as a function of the coordinates of the proton $(u'=0, x')$. This is given, according to the Hellmann-Feynaman theroem, by

$$W(x') = V_0(x') + \tfrac{1}{2}\bar{V}_1(x=x', u=0), \tag{5.1}$$

where $V_0(x')$ is the electrostatic potential of the "bare" surface and $\bar{V}_1(x=x', u=0)$ is the potential of the screening charge evaluated at the proton location. The latter can be obtained from $V_1(x,x';u)$, since

$$\bar{V}_1(x,x';u) = V_1(x,x';u) - [(x-x')^2+u^2]^{-1/2} \ .$$

The results are shown in Fig. 1. In Sec. IV, we have established that for large $x'$, $W(x')$ tends to the image potential, i.e.,

$$W(x') \underset{x'\to\infty}{\longrightarrow} 1/[4(x'-x_0)] \ , \tag{5.2}$$

where $X_0 = \int x n_1(u,x;x'=\infty)\, d\vec{r}$. As $x'$ approaches the surface region ($x \leq 5$ a.u.), the interaction energy begins to deviate significantly from the image potential as shown in Fig. 1. Finally a minimum in $W(x')$ is reached at $x' \simeq 1.08$ a.u. The minimum results from a competition between the repulsive term $V_0(x')$ and the attractive term $\frac{1}{2}\bar{V}_1(x=x', \mu=0)$. While the position of the minimum can be used to locate the nucleus of chemisorbed hydrogen (at least at low temperatures), the curve is rather broad near the minimum. Thus we have included a rea-

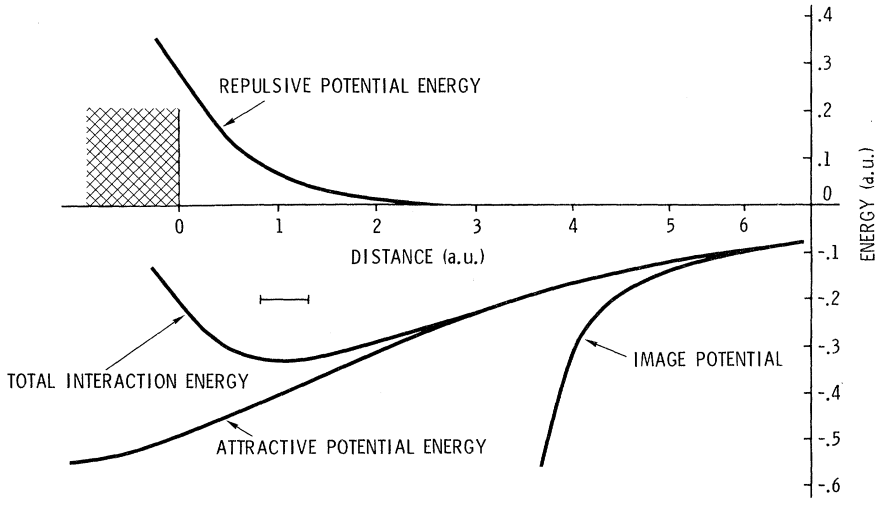


FIG. 1. Hydrogen-ion–metal interaction energy versus separation distance. The nucleii of the surface plane of the metal are located at $-d/2$, where $d$ is the distance between planes parallel to the surface.

sonable error bar. The depth of the minimum gives the ionic desorption energy, $E_I = 9$ eV. The experimental value[21,22] for hydrogen on tungsten is $E_I \simeq 11.3$ eV. This gives one a measure of the accuracy of the calculation. For a first-principles calculation with no adjustable parameters, this sort of agreement is encouraging. It should be added that experimentally hydrogen is singular in that its ionic desorption energy is much larger than that of other chemisorbed species. This is borne out by our calculation.

The *atomic* desorption energy of hydrogen is 3.0 eV while from our calculated *ionic* desorption energy one deduces (see Ref. 21) a value of $9.0 + 5.3 - 13.6 = 0.7$ eV, too small by a factor of 4. Thus the 20% error in the calculated ionic desorption energy becomes greatly magnified, and our method, which, by its nature, yields the ionic desorption energy as the primary result, does not have enough precision for an accurate subsequent calculation of the atomic desorption energy.

### B. Vibrational frequency

The adsorbed hydrogen will exhibit vibrational modes in the potential well of Fig. 1. The excitation energy is given by

$$\hbar\omega = \hbar\left(\frac{1}{m}\frac{d^2W(x)}{dx^2}\right)^{1/2}_{x_m} , \tag{5.3}$$

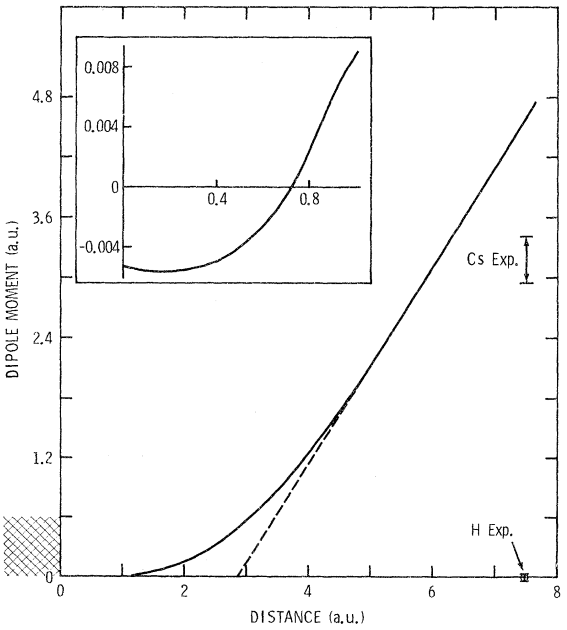


FIG. 2. Hydrogen-adatom dipole moment versus the distance between the proton and the metal substrate. The Cs experimental results were taken from those compiled in Ref. 20, while the H experimental results are from Ref. 17.

where $x_m$ is the coordinate of the proton at its energy minimum (1.08 a.u.), and $m$ is the proton mass. The theoretical value of 200 meV is to be compared with the 140-meV experimental result.[17,23] This fair agreement between the single-adsorbate theoretical result and experiment is consistent with dissociative adsorption.

### C. Adatom interaction

One can investigate the question of molecular versus atom adsorption also by determining the short-range ($\leq 2$ a.u.) interaction energy between hydrogen adatoms.

One can again use the Hellmann-Feynman theorem to show that $V_1(x, x', u)$ is the interaction energy between adatoms whose nuclei are located at $(x, u)$ and at $(x', 0)$, respectively. We found that for representative $x'$ values, the short-range interaction energy is repulsive. This is to be contrasted with gaseous hydrogen, which has an interaction energy minimum[25] at a separation of 1.4 a.u. Thus we have further evidence of dissociative adsorption. This supports the numerous experimental contentions (see, e.g., Ref. 16) that hydrogen dissociates upon adsorption in the first adlayer on tungsten and certain other metals.

### D. Dipole moment—comparison with Cs

The dipole moment of the chemisorbed hydrogen is given by

$$P = \int (x' - x) n_1(\vec{r})\, d\vec{r}, \tag{5.4}$$

shown in Fig. 2 as a function of $x'$, the location of the hydrogen nucleus. At large separations, since the screening charge remains in the metal [see Eq. (4.9)],

$$P \underset{x' \to \infty}{\longrightarrow} (x' - x_0) \ . \tag{5.5}$$

Equation (5.5) is exhibited by the dashed line in Fig. 2. The intercept of this line with the abscissa gives the image-plane location $x_0$. We believe that our calculated distance $x_0$ of the image plane from the jellium surface is too large. This is discussed in detail in Appendix A. It is likely, however, that the image plane lies on the vacuum side of the chemisorbed H, that is, $x_0 > 1.08$ a.u.

As the positive charge is moved from the outside to smaller $x'$, it "catches up" with its screening charge. This leads to a decrease in $P$, as shown in Fig. 2. In fact, our calculation gives a change in sign of $P$, as shown in the inset of Fig. 2. This change in sign occurs in the vicinity of the energy minimum of Fig. 1, i.e., the equilibrium position of the chemisorbed H. This may shed some light on why the dipole moment of chemisorbed H on W (110) is positive whereas it is negative on W(100) (see Ref. 17 for a discussion of this). One would expect

the equilibrium position on these two planes to be different.

However, one should not take our results in the inset too seriously. It is shown in Appendix C that at $x' = 0$ the dipole moment is, in fact, exactly zero. Thus our error there is $\cong 5\times10^{-3}$ a.u. This led us to test the sensitivity of $P$ to our various approximations. First, we tested the sensitivity to $n_0(x)$. The results in Fig. 2 were obtained using the numerical solution by Warner[26] to the zero-order Euler equation [Eq. (2.5)]. In Ref. 10, Fig. 2, $P$ as obtained using Lang and Kohn's $n_0(x)$ is plotted. A comparison shows that these two slightly different zero-order solutions lead to a difference in the dipole moment of order $10^{-2}$ a.u. Thus small inaccuracies in $n_0(x)$ are the likely source of the aforementioned error at $x' = 0$. This is contrary to the behavior of the desorption energy, which was found to be relatively insensitive to small changes in $n_0(x)$. Likewise the sensitivity of $P$ to the coefficient of the inhomogeneity term in the energy functional [Eq. (3.6)] is much greater than that found for the desorption energy (see Appendix A).

Thus the only conclusion we can draw from our calculations is that the dipole moment of H is very small, of order $10^{-2}$ a.u. This is consistent with experiment. From Eqs. (5.5) and (4.9), one sees that $P$ is equal to the shift of the center of mass of the screening charge relative to the proton. Thus for hydrogen, this shift is only of the order of $10^{-2}$ of a Bohr radius.

By contrast, for Cs this shift is much larger, approximately 2.9 to 3.4 a.u.[20] as shown in Fig. 2. As a check of our $P(x')$ plot and an illustration of the use of our response function, we make an approximate calculation of the Cs dipole moment in the limit of zero coverage. Following Lang,[20] we represent the Cs adlayer very approximately by a slab of jellium from $x = 0$ to 8.08 a.u. In general, the dipole moment is given by

$$\int P(x')\rho_1^{ex}(\vec{r}')\,d\vec{r}', \tag{5.6}$$

where $P(x')$ is shown in Fig. 2. For Lang's slab model, the dipole moment is simply the average of $P(x')$ over the thickness of the slab. The resultant dipole moment is 2.07 a.u., about 30% low. Note that this result is two orders of magnitude larger than the H dipole moment.

### E. Charge distribution and differential scattering cross sections

The "shape" of the adsorbed hydrogen (proton plus screening charge distribution) changes rapidly as a function of proton position, as shown in Fig. 3 (see also Fig. 3 of Ref. 10). When the hydrogen is located at the energy minimum [Fig. 3(a)], it is nearly spherically symmetric (small dipole moment). However, when the proton has been moved only 1.72 Å in the direction of the vacuum [Fig. 3(b)], the adatom is quite asymmetric, resulting in a large dipole moment (cf. Fig. 2). Further, the screening charge spreads in the direction parallel to the surface, that is, in the $u$ direction. The ratio of the peak $n_1$ values between Figs. 3(a) and 3(b) is $\simeq 13$.

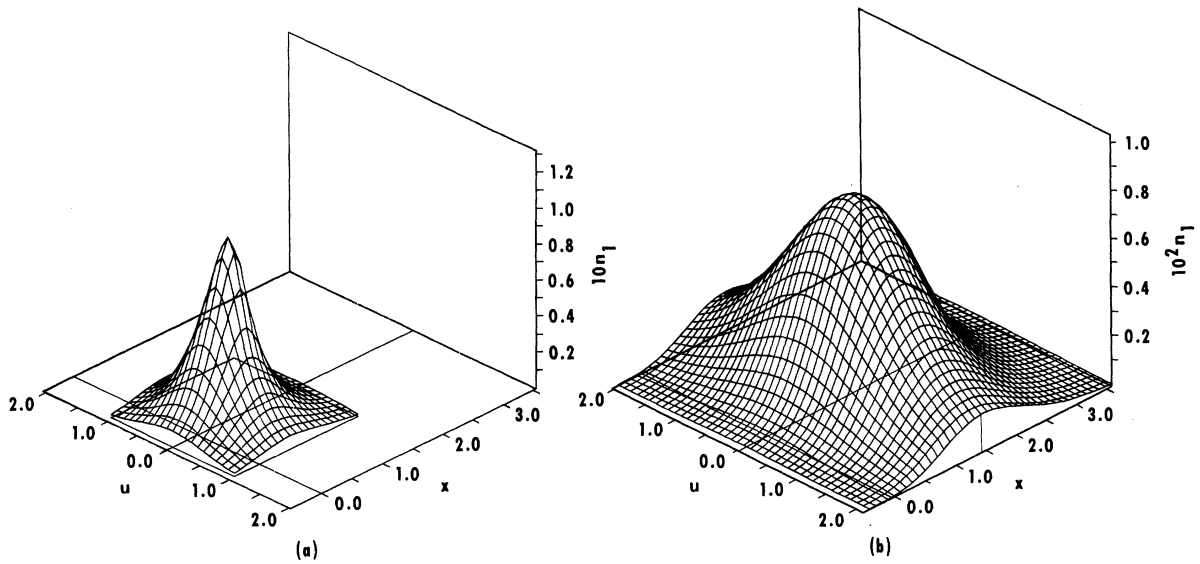


FIG. 3. Screening charge density $n_1$ for two proton positions: (a) at $u = 0$, $x = 0.571$ Å, the interaction energy minimum, i.e., the location for chemisorbed H; (b) at $u = 0$, $x = 2.29$ Å, a small displacement in the vacuum direction from the adsorption site. $u$ is the cylindrical coordinate in the plane parallel to the surface measured from an axis through the proton. Scaled units (Ref. 9) are used for $n_1$. $x$ and $u$ are given in Å. The vertical line denotes the $n_1$ peak location.

At the energy minimum, the screening charge density at the proton in Fig. 3(a) is only 0.36 of that of an isolated hydrogen atom. Thus one expects that chemisorbed hydrogen will scatter electrons more strongly than does atomic hydrogen. We will see that this is in fact the case.

When hydrogen is introduced onto a clean W(100) surface, a $c(2\times 2)$ low-energy-electron-diffraction (LEED) pattern is observed[18] which exhibits additional (half-order) beams. The intensity of these extra beams is comparable to the other (integral order) beams of the pattern. The result is made more interesting by the fact that the back scattering cross sections of an isolated hydrogen atom are an order of magnitude smaller than those of the W atom[27] in the 50–100-eV energy range. Analogous data have been obtained for other light absorbates on heavy substrates. The interpretation has been somewhat controversial. Some authors[28] feel these data indicate reconstruction of the substrate, while others[29] feel that reconstruction is not a necessary condition. More recently, Jennings and McRae[30] have shown that in this system interlayer multiple scattering can lead to fractional-order beams of intensity comparable to neighboring integral-order beams, when isolated H-atom phase shifts are used. In the following we shall show the effect of chemisorption on the differential scattering cross sections (DCS) of hydrogen.

A DCS calculation directly involves the potential well at the adsorbate. In Fig. 4 we've plotted $RV_1(\vec{r})$, where $R=[(x-x')^2+u^2]^{1/2}$. Note that this electrostatic potential is nearly spherically symmetric. $V_1(r)$ is spherically symmetrized so that standard atomic-physics methods can be applied to the DCS calculation. This is analogous to the potential (atomic units are used throughout unless

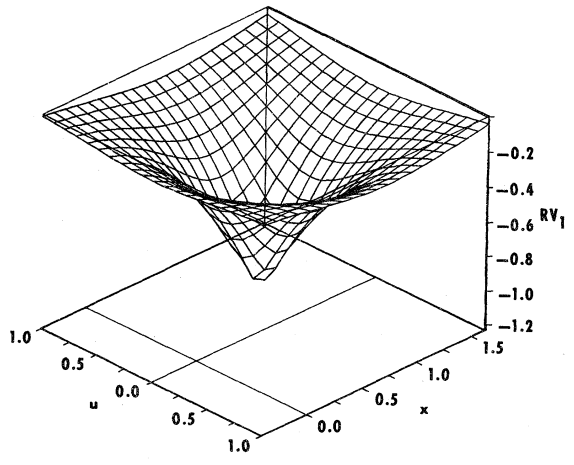


FIG. 4. Screened electrostatic potential of the proton multiplied by $R=[(x-x')^2+u^2]^{1/2}$. The proton is located at $x'=0.571$ Å. $RV_1$ is in a.u., while $x$ and $u$ are in Å.

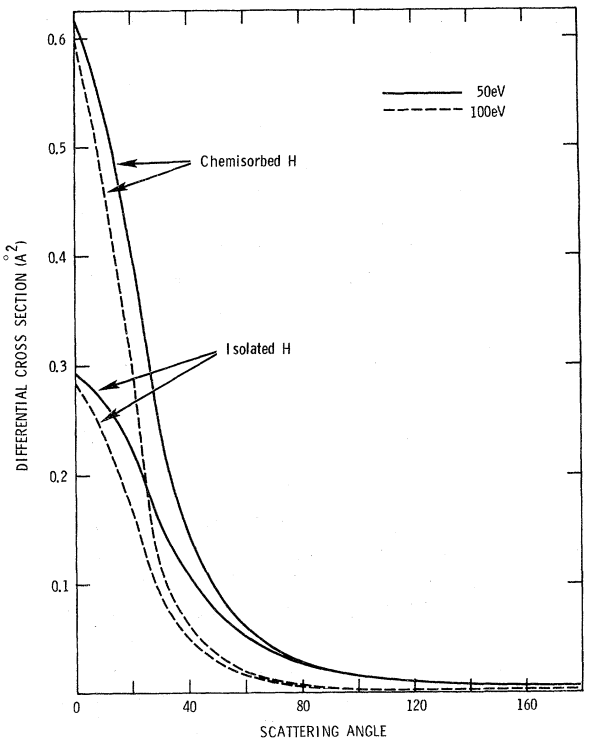


FIG. 5. Differential scattering cross sections for chemisorbed and isolated hydrogen atoms. The chemisorbed atom is located at the energy minimum of Fig. 1.

noted otherwise)

$$V_A(r)=(1+1/r)e^{-2r} \tag{5.7}$$

used for the isolated H atom. Exchange between the incident and atomic electron and polarization effects have been shown[31] (see also Ref. 32) to be relatively unimportant ($\lesssim 20\%$) to the scattering cross section of atomic H for incident energies $\gtrsim 50$ eV. These effects are ignored in our calculation for both atomic and chemisorbed hydrogen. The scattering phase shifts were determined by numerical integration of the Schrödinger equations formed from the potentials $\langle V_1(\vec{r})\rangle$ and $V_A(r)$, respectively. Eleven phase shifts were included in our DCS calculation for both the isolated and chemisorbed particle.

The results are shown in Fig. 5. The backscattering (large scattering angle) DCS at either 50 or 100 eV are imperceptibly changed by chemisorption, and thus remain very small. However, as the scattering angle decreases, chemisorption substantially increases the DCS.[33] Our results appear to support the picture of Jennings and McRae, but one would have to do a multiple scattering calculation using our DCS (or, equivalently, our phase shifts) to be certain. Figure 5 exhibits, for the first time to our knowledge, the effect of chemisorption on a DCS. We expect that such

considerations may be useful in LEED adsorbate crystallography.

### F. Resonance level

Recent photoemission data[10,11] has shown a change in the surface density of states of W(100) upon hydrogen chemisorption. It is interesting then to look for possible resonance levels associated with a hydrogen adatom. We write the total effective potential $v(\vec{r})$ of the system (W + H) as the potential $v_0(x)$ of bare W plus a remainder:

$$v(\vec{r}) = v_0(x) + v_1(\vec{r}), \tag{5.8}$$

where

$$\begin{aligned} v(\vec{r}) &= -V(\vec{r}) - (3/\pi)^{1/3} n^{1/3}(\vec{r}), \\ v_0(x) &= -V_0(x) - (3/\pi)^{1/3} n_0^{1/3}(x), \end{aligned} \tag{5.9}$$

and $V$ and $n$ stand, respectively, for electrostatic potentials and electron densities. The potential $v(\vec{r})$ is plotted in Fig. 6. There the proton is located at $x = 0.571$ Å, $u = 0$, the interaction energy minimum. For negative $x$, one can notice a "lip" which is an indication that the potential is dropping down to its bulk value inside the metal.

In keeping with the small dipole moment it is found that $v_1(\vec{r})$ is nearly spherically symmetric and may be replaced by its spherical average. The center of the resonance level can now be found quite simply. First, the bound-state spectrum of a spherically symmetrized $v_1(\vec{r})$ is obtained numerically. It turns out that there is only one bound state. This $s$ level is then shifted downward by $v_0(x_m)$, where $x_m$ is the coordinate of the proton at its energy minimum (Fig. 1). The result is that the resonance level $\epsilon_1$ lies 5.6 below the Fermi level.

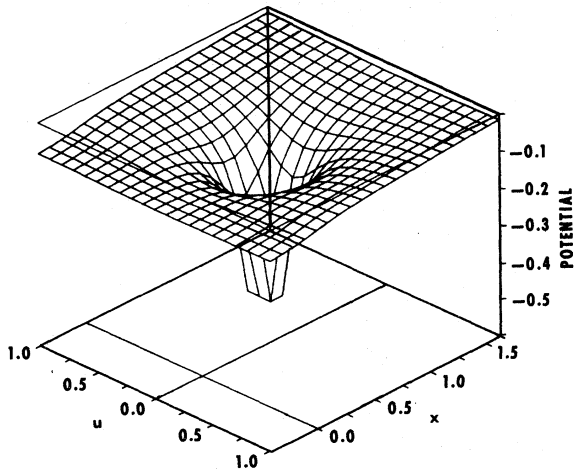


FIG. 6. Total electronic potential in the vicinity of the chemisorbed hydrogen, $v(\vec{r})$, Eqs. (5.8) and (5.9). The potential is in a.u., while $u$ and $x$ are in Å.

Plummer and Waclawski[34] show a peak in their difference spectra for hydrogen adsorption at 5.7 and 6.3 eV below the Fermi level for W(100) and W(110), respectively (see also Ref. 35). The agreement between theory and experiment indicates that these low-lying states are localized primarily on the adsorbate (compare with Ref. 8).

We have also calculated the width of this resonance level in the Hartree-Fock approximation to the Anderson[36] Hamiltonian. In this model, the width of the resonance level $\Gamma$ is given by

$$\Gamma = \pi \rho(\epsilon_1) \langle |V_{1k}|^2 \rangle_{\epsilon_1} \tag{5.10}$$

where $\rho(\epsilon_1)$ is the substrate density of states,

$$\langle |V_{1k}|^2 \rangle_{\epsilon_1} = \left\langle \left| \int \Psi_{\vec{k}}^*(\vec{r}) v_1(r) \Psi_1(\vec{r})\, d\vec{r} \right|^2 \right\rangle_{\epsilon_1}$$

is the mean-square coupling matrix element of the spherically symmetrized perturbing potential $v_1(r)$ between substrate (unperturbed) wave functions $\Psi_{\vec{k}}^*(\vec{r})$ and bound-state wave function $\Psi_1(\vec{r})$. We find a half-width $\Gamma$ equal to 2.7 eV which is to be compared with an experimental value of $\lesssim 1$ eV. The discrepancy may reflect the limitations of our model, or inherent inaccuracies in applying the result in Eq. (5.10) to the chemisorption system.[37]

It is often remarked in the literature that a condition for validity of a molecular-orbital approach to chemisorption is $\pi\Gamma \geq U$, where $U$ is the effective intra-atomic interaction energy on the hydrogen atom, whose value is generally estimated to be 5–10 eV. Using the experimental level width, one finds that this inequality is seriously violated. However, the fairly good over-all agreement with experiment which we obtained suggests this inequality may be too strong a condition for the validity of the density-functional formalism. This is also suggested by theoretical considerations of the separated-atom limit,[38] for which the density-functional formalism gives the correct energy.

## VI. SUMMARY

In this paper we have used the density functional formalism for a first, exploratory theoretical study of chemisorption. The system to which the theory was applied is hydrogen on tungsten, which has been well investigated experimentally. In our calculation three types of approximations have been made: (i) representation of the substrate by a jellium model, (ii) a simple form of the density functional, and (iii) treatment of the effects of the adatom by linear-response theory. Qualitative considerations suggest that none of these approximations is unreasonable for the problem at hand. It is noteworthy that agreement between our theory and experiment, as summarized in Table I for several physical properties of this system, is quite good.

If linear-response theory is indeed at least semiquantitatively useful for certain chemisorption systems, our formalism may have a rather wide usefulness. For example, the effect of the actual crystal ions can be easily included in the theory, provided they are regarded as a small perturbation susceptible to linear-response theory. Similarly the adsorption of other atoms, such as the alkalis, can be studied by this theory. Such calculations are currently in progress.

At the same time we consider it very important that improvements on all our approximations be carried out so that the theory can be put on a firmer and more quantitative basis.

## ACKNOWLEDGMENTS

The authors would like to thank Dr. Ward Plummer for sending his data prior to publication and for many helpful conversations. We are also grateful for comments on various aspects of this work by Dr. Norton Lang and Dr. J. C. Tracy, and for the programming assistance of J. C. Price.

## APPENDIX A

This appendix is devoted to further discussion of the linear approximation and an investigation of the validity of keeping a single inhomogeneity term of the form $(\nabla n)^2/n$ in the energy functional (3.6).

It was noted in the text just prior to Eq. (3.7) that the surface calculation of Appelbaum[14] and Hamann indicated that the linear approximation is rather good for interaction-energy calculations in the case of chemisorption. Sjölander[39] and Stott considered the bulk screening of a positron, and found the linear approximation to be inadequate for determining the positron-electron static pair correlation function near the positron. Of course the conclusions of these two papers are not necessarily in disagreement, because of the different quantities considered—binding energies versus correlation functions. More importantly, perhaps, a surface calculation was done in Ref. 14 while only bulk screening was considered in Ref. 39. One of the main results of our work is that surface screening depends rather sensitively on the location of the proton in the surface. This is consistent with the fact that the unperturbed electron density $n_0(x)$ in the vicinity of the proton is decreasing in the vacuum direction.

Another approximation was the keeping of a single inhomogeneity term in Eq. (3.6). Again it is important to investigate this approximation in a surface calculation rather than a bulk (homogeneous) calculation.

This approximation has been analyzed for other systems by a number of authors.[40] A recent work by Jones and Young[40] is particularly relevant for our purpose. These authors evaluated the linear-response function for a bulk metal in both the random-phase approximation and the density-functional theory with an inhomogeneity term of the form $\frac{1}{8}\lambda(\nabla n)^2/n$. The response function for a uniform electron gas is defined as $F(q)=n_1(q)/V_1(q)$, where $F(q)$ is given as

$$F(q)=-\frac{k_f}{\pi^2}\frac{1}{2}\left(1+\frac{1-\eta^2}{2\eta}\ln\left|\frac{1+\eta}{1-\eta}\right|\right) \tag{A1}$$

in random-phase approximation (RPA), and

$$F(q)=-\frac{k_f}{\pi^2}\frac{1}{1+3\lambda\eta^2} \tag{A2}$$

in the density-functional approach; here $\eta=q/2k_f$.

For small $\eta$, the choice of $\lambda=\frac{1}{9}$ corresponding to the leading gradient expansion in the energy functional [as in Eq. (3.6)] gives the correct leading terms for $F(q)$ in powers of $\eta^2$, whereas for large $\eta$ the value of $\lambda=1$, known as the von Weizacker term (obtained from variational consideration) gives the correct leading terms in powers of $1/\eta^2$. Thus if one were to use $\lambda=\frac{1}{9}$, one would expect the screening charge density to be relatively inaccurate near the proton (large $q$) and relatively accurate far from the proton (small $q$). For quantities which are determined by an integration of a density functional over all of configuration space, the accuracy would depend on the average $\eta$.

Examples of such quantities are those computed in this paper: ionic desorption energy, resonance level, dipole moment, etc. One can find an average $\eta$ and estimate the applicability of gradient expansion to surface response theory. To accomplish this, an effective $\lambda$ was determined for the charge cloud around the proton at equilibrium position in the surface, by evaluating

$$\langle q\rangle=\frac{\int_{-\infty}^{\infty}|Q_x n_1(Q_x)|dQ_x}{\int_{-\infty}^{\infty}|n_1(Q_x)|dQ_x}\ , \tag{A3}$$

$$\langle n_0\rangle=\int_{-\infty}^{\infty}n_0(x)n_1(Q=0,x)dx\ , \tag{A4}$$

$$\langle k_f\rangle=(3\pi^2)^{1/3}\langle n_0\rangle^{1/3}\quad\text{and}\quad\langle\eta\rangle=\langle q\rangle/2\langle k_f\rangle\ , \tag{A5}$$

where

$$n_1(Q_x)\equiv\int_{-\infty}^{\infty}e^{-iQ_x x}n_1(Q=0,x)dx\ . \tag{A6}$$

For the adsorbed hydrogen at the equilibrium position it is found that $\langle n_0\rangle=9.52\times10^{-3}$, which corresponds to a local $r_s$ of 2.9, and $\langle\eta\rangle=0.72$.

Referring back to (A1) and (A2), we see that the choice of $\lambda=0.16$ would make the response function in the density-functional theory agree with the corresponding value in RPA. This is much closer to $\lambda=\frac{1}{9}$ than it is to $\lambda=1$. When we carried out the calculation in the text for $\lambda=0.16$, the result for the binding energy was changed by only a few per-

cent, showing that the effect of the higher-order gradient corrections in the kinetic-energy functional is small. The location of the image plane $x_0$, however, is quite sensitive to the choice of $\lambda$, varying between 3.2 and 1.9 a.u. for $\lambda$ between $\frac{1}{9}$ and $\frac{1}{3}$. Since the image plane is determined by asymptoptic quantities when the proton is far out in the tail region, we expect the effective $\lambda$ for this quantity determined via (A3) and (A4) is larger than 0.16, thus locating the image plane closer to 1.9 a.u. from the jellium surface, as found by Lang and Kohn,[15] who treated the kinetic-energy functional exactly.

## APPENDIX B

We examine here the consequences of including the correlation energy contributions in $g_0(n)$ and $g_2(n)$. First, the terms in $g_2(n)$ due to exchange and correlation are[41,42]

$$g_2^x = -0.00167 n^{-4/3}\,, \qquad g_2^c = 0.00424 n^{-4/3}\,, \tag{B1}$$

which is much smaller than the kinetic-energy contributions $\frac{1}{72}(\nabla n)^2/n$ at an electronic density corresponding to $r_s = 1.5$. Further, Hedin *et al.*[43] have found that the local-density approximation in exchange and correlation gives very good agreement with the dielectric functions of Singwi *et al.*[44] and Geldardt and Taylor.[45] Thus the neglect of the gradient terms appears to be a good approximation. As to the correlation contribution to $g_0(n)$, a form that has been frequently employed is the Wigner interpolation formula

$$g_0^c(n) = -\int \frac{0.056 n^{4/3}}{0.079 + n^{1/3}}\, d\vec{r}\,. \tag{B2}$$

Inclusion of this term in $g_0(n)$ is straightforward with the present formalism. The only change is that in the basic equation (3.14) in the text, the quantity $Y$ is now changed to the form

$$Y = \left(\frac{n_0'(x)}{n_0(x)}\right)^2 - \frac{n_0''(x)}{n_0(x)} + \tfrac{9}{2} n_0^{1/3}(x) - \tfrac{2}{3} k_h n_0^{2/3}(x) + 0.014\, \frac{0.41 n_0^{2/3}(x) + 0.16 n_0^{1/3}(x)}{[0.079 + 0.41 n_0^{1/3}(x)]^3}\,. \tag{B3}$$

The resultant potential energy curve for the chemisorbed hydrogen is not appreciably changed from the one given in Fig. 1. The ionic desorption energy is changed by only about 2% while the position of the image plane is shifted outward by 8%.[46]

## APPENDIX C

It was stated in the text that the hydrogen dipole moment is exactly zero when $x' = 0$ (proton at the jellium surface). This is a general result of linear-response theory, independent of the approximation to $G[n]$. This conclusion is derived in the following.

From Eq. (5.4), only the $Q = 0$ Fourier component of $n_1$ contributes to $P$. Thus one need only deal with the $Q = 0$ Fourier component of the perturbing point charge $\rho_1^{\rm ext}(\vec{r}')$, which is a charged sheet, $z\,\delta(x - x')$. Since we deal in *linear* response, we compute the dipole moment for $\lim(z) \to 0$. Such a charged sheet can be formed from a slab of density $\rho_+$ (jellium density) filling the space between $0 \le x' \le \Delta x_1$, by taking $\lim \Delta x_1 \to 0$. Then the dipole moment per unit perturbing charge is given by

$$\lim_{z\to 0}(P/z) = \lim_{\Delta x_1 \to 0} \frac{1}{4\pi\rho_+}\,\frac{\Delta\phi_e}{\Delta x_1}\,, \tag{C1}$$

where $\Delta\phi_e$ is the change in electron work function due to the introduction of the slab.

Now a slab of density $\rho_+$ added contiguously to the surface of a jellium of the same density merely thickens the metal, without changing the shape of the electronic charge distribution. Thus $\Delta\phi_e$ is zero for all $\Delta x_1$, and so

$$\lim_{z\to 0}(P/z) = 0\,, \tag{C2}$$

which is the desired result.

---

*Alfred P. Sloan Foundation Research Follow; supported in part by the National Science Foundation under Contract No. GH37782 and the Material Science Program at Brown University.

†Supported in part by the Office of Naval Research and the National Science Foundation.

[1]J. W. Gadzuk, in *Surface Physics of Crystalline Solids*, edited by J. M. Blakeley (Academic, New York, 1974); R. Gomer, S. Lyo, and J. Smith, in *Interactions on Metal Surfaces*, edited by R. Gomer (Springer-Verlag, Berlin, 1975).

[2]D. M. Newns, Phys. Rev. 178, 1123 (1969).

[3]T. B. Grimley, J. Phys. C 3, 1934 (1970). See also A. Madhukar, Phys. Rev. B 8, 4458 (1973).

[4]A. J. Bennett and L. M. Falicov, Phys. Rev. 151, 512 (1966).

[5]T. Einstein and J. R. Schrieffer, Phys. Rev. B 7, 3629 (1973).

[6]F. Cyrot-Lackmann, J. Vac. Sci. Technol. 9, 1045 (1972).

[7]J. R. Schrieffer and R. Gomer, Surf. Sci. 25, 315 (1971).

[8]L. W. Anders, R. S. Hansen, and L. S. Bartell, J. Chem. Phys. 10, 5277 (1973).

[9]S. C. Ying, J. R. Smith, and W. Kohn, J. Vac. Sci. Technol. 9, 575 (1971).

[10]See J. R. Smith, S. C. Ying, and W. Kohn, Phys. Rev. Lett. 30, 610 (1973); Solid State Commun. 15, 1491 (1974).

[11]P. Hohenberg and W. Kohn, Phys. Rev. 136, B864 (1964).

[12]J. R. Smith, Phys. Rev. 181, 522 (1969).

[13]N. Lang and W. Kohn, Phys. Rev. B 1, 4555 (1970).
[14]J. Appelbaum and D. Hamann, Phys. Rev. B 6, 1122 (1972).
[15]N. Lang and W. Kohn, Phys. Rev. B 7, 3541 (1973).
[16]T. E. Madey, Surf. Sci. 36, 281 (1973).
[17]E. W. Plummer and A. E. Bell, J. Vac. Sci. Technol. 9, 583 (1972).
[18]K. Yonehara and L. D. Schmidt, Surf. Sci. 25, 238 (1971); P. J. Estrup and J. Anderson, J. Chem. Phys. 45, 2254 (1966).
[19]B. J. Hopkins and S. Usami, Surf. Sci. 23, 423 (1970).
[20]N. Lang, Phys. Rev. B 4, 4234 (1971).
[21]The experimental $E_1$ is obtained from the atomic desorption energy $E_a$, the hydrogen ionization potential $I$, the electron work function $\phi_e$, and the Born-Haber cycle: $E_I = E_a + I - \phi_e$. $E_a$ appears not to be very sensitive to the surface plane, and we used a representative value of 70 kcal/mole (see Ref. 22.) As mentioned earlier, the model is most appropriate to a close-packed plane, and therefore we took $\phi_e = 5.3$ eV.
[22]See, e.g., T. E. Madey and J. T. Yates, Jr., *Structure et Properties des Surface des Solides* (Editions du Centre National de la Recherche Scientifique, Paris, 1970), No. 187, p. 155; T. W. Hickmott, J. Chem. Phys. 32, 810 (1960).
[23]F. M. Propst and T. C. Piper, J. Vac. Sci. Technol. 4, 53 (1967).
[24]The energy of vibration of molecular hydrogen is 550 meV, according to G. Herzberg, *Molecular Spectra and Molecular Structure. I. Spectra of Diatomic Molecules*, 2nd ed. (Van Nostrand, New York, 1963).
[25]See, e.g., S. Raimes, *The Wave Mechanics of Electrons in Metals* (North-Holland, Amsterdam, 1974).
[26]C. Warner, in Proceedings of the IEEE Thermionic Specialists Conference, 1971 (unpublished).
[27]M. Fink and A. C. Yates, At. Data (to be published).
[28]See, e.g., L. H. Germer, Surf. Sci. 5, 147 (1966).
[29]See, e.g., E. Bauer, Surf. Sci. 5, 152 (1966); J. C. Tracy and J. M. Blakely, Surf. Sci. 15, 257 (1969).
[30]P. J. Jennings and E. G. McRae, Surf. Sci. 23, 363 (1970).
[31]H. S. W. Massey and B. L. Moiseiwitsch, Proc. R. Soc. Lond. 205, 483 (1950).
[32]D. Gregory and M. Fink, Phys. Rev. A 7, 1251 (1973); M. Fink, M. R. Martin, and G. A. Somorjai, Surf. Sci. 29, 303 (1972); R. A. Bonham, Phys. Rev. A 3, 298 (1971).
[33]The chemisorbed-H DCS at 50 eV were also computed in the Born aprpoximation as a check. The Born DCS are slightly smaller than those of Fig. 2, but the difference is $\leq 0.008$ Å$^2$ for selected angles throughout the range.
[34]E. W. Plummer and B. J. Waclawski, Proceedings of the Physics and Electronics Conference, 1973 (unpublished); E. W. Plummer (unpublished).
[35]B. Feurebacher and B. Fitton, Phys. Rev. B 8, 4890 (1973).
[36]P. W. Anderson, Phys. Rev. 124, 41 (1961).
[37]J. W. Gadzuk (Ref. 1); A. Madhukar (Ref. 3). These authors choose the matrix element in Eq. (5.10) so that the Hartree-Fock approximation to the Anderson Hamiltonian gives the observed desorption energy. They then find that $\Gamma$ is several volts, similar to our results. Madhukar argues that the error in $\Gamma$ is due in part to the lack of orthogonality between adatom and metal wave functions, which is not properly accounted for in the Anderson Hamiltonian.
[38]J. C. Slater and K. H. Johnson, Phys. Rev. B 5, 844 (1972).
[39]A. Sjölander and M. J. Stott, Phys. Rev. B 5, 2109 (1972).
[40]W. Jones and W. H. Young, J. Phys. C 4, 1322 (1971); C. H. Hodges, Can. J. Phys. 51, 1428 (1973); D. A. Kirzhnits, Zh. Eksp. Teor. Fiz. 32, 115 (1956) [Sov. Phys.-JETP 5, 64 (1957)]; and N. N. Kalitkin, Zh. Eksp. Teor. Fiz. 38, 1534 (1960) [Sov. Phys.-JETP 11, 1106 (1960)].
[41]L. J. Sham, in *Computational Methods in Band Theory*, edited by P. M. Marcus *et al.* (Plenum, New York, 1971).
[42]S. K. A. Ma and K. A. Brueckner, Phys. Rev. 165, 18 (1968).
[43]L. Hedin, B. Lundquist, and S. Lundquist, Solid State Commun. 9, 537 (1971).
[44]K. S. Singwi *et al.*, Phys. Rev. B 1, 1044 (1970).
[45]D. J. W. Geldart and R. Taylor, Can. J. Phys. 48, 167 (1970).
[46]Very recent work [J. Harris and R. O. Jones, Phys. Lett. A 46, 407 (1974)] suggests that surface correlation effects are much larger than those obtained from Eq. (B2).